Developmental Cell, Vol. 1, 265–275, August, 2001, Copyright ©2001 by Cell Press

Growth and Function of the Embryonic Heart Depend upon the Cardiac-Specific L-Type Calcium Channel α1 Subunit

Wolfgang Rottbauer,[1] Keith Baker,[2] Z. Galen Wo,[1] Manzoor-Ali P.K. Mohideen,[1,4] Horacio F. Cantiello,[1] and Mark C. Fishman[1,3]
[1] Department of Medicine
[2] Department of Anesthesia
Harvard Medical School
Massachusetts General Hospital
Boston, Massachusetts 02114

Summary

The heart must function from the moment of its embryonic assembly, but the molecular underpinnings of the first heart beat are not known, nor whether function determines form at this early stage. Here, we find by positional cloning that the embryonic lethal *island beat* (*isl*) mutation in zebrafish disrupts the α1C L-type calcium channel subunit (C-LTCC). The *isl* atrium is relatively normal in size, and individual cells contract chaotically, in a pattern resembling atrial fibrillation. The ventricle is completely silent. Unlike another mutation with a silent ventricle, *isl* fails to acquire the normal number of myocytes. Thus, calcium signaling via C-LTCC can regulate heart growth independently of contraction, and plays distinctive roles in fashioning both form and function of the two developing chambers.

Introduction

Voltage-gated calcium entry across the plasma membrane of excitable cells is accomplished via calcium-permeable ion channels. In the adult heart, calcium entry is an essential element of the heart beat, contributing to pacemaking, action potential, conduction, and excitation-contraction (EC) coupling (Marban, 1999). Additionally, by less clear mechanisms, calcium regulates cellular growth and hypertrophy (Hermsmeyer et al., 1997; MacLellan and Schneider, 2000; Frey et al., 2000).

L-type calcium channels (LTCCs) comprise the predominant route for calcium entry into cardiac myocytes. LTCCs are heteromultimeric complexes that are activated by strong depolarization and sensitive to dihydropyridine blockade. The ion-conducting pore of the LTCC lies in its α1 subunit. There are different α1 subunits of LTCCs in vertebrates, termed α1F, α1S, α1D, and α1C. The predominant cardiac isoform is α1C (reviewed in Striessnig, 1999).

The role of LTCCs in the development of embryonic cardiac form and function is unclear. Because of the relative paucity of sarcoplasmic reticulum in embryonic cardiocytes, L-type calcium currents contribute proportionally more to the EC coupling in the embryo than in the adult (Brotto and Creazzo, 1996; Ramesh et al., 1995). Thus, LTCC blockers, such as 1,4-dihydropyridine, disrupt heart growth in chick embryos such that the size of the heart and thickness of the myocardium are reduced (Sedmera et al., 1998). However, targeted mutagenesis of the LTCC α1C subunit ($Ca_v1.2$), the most prominent in the mouse heart, was recently reported not to disrupt earliest embryonic cardiac function and morphogenesis (Seisenberger et al., 2000), while mutation of the α1S subunit, predominant in skeletal muscle, exerts a strong effect on skeletal muscle form and function, leading to paralysis and muscular dysgenesis in mice (Chaudhari, 1992).

In mammals, it is difficult to interpret the developmental and functional impact of mutations in genes essential for embryonic cardiac function because embryonic survival and tissue integrity are largely dependent upon blood flow, such that form and function are inextricably intertwined. However, zebrafish embryos live by diffusion for several days (Pelster and Burggren, 1996), and so heart function is largely "dispensable."

island beat (*isl*) is an ethylnitrosourea (ENU)-induced, embryonic lethal recessive mutation in zebrafish, which selectively perturbs cardiac morphogenesis and function in early embryonic development (Stainier et al., 1996). The *isl* ventricle fails to grow and does not contract, while the atrium exhibits rapid, isolated, and discoordinated contractions. By positional cloning, we identified the *isl* mutations as in the gene for the pore-forming α1C subunit of the LTCC. These mutations abolish L-type calcium currents in *isl* cardiomyocytes. As a consequence, the ventricle fails to grow and is electrically silent. In contrast, wild-type cells transplanted to *isl* ventricles can beat, but only when several wild-type cells are in clusters. This indicates that LTCC activity contributes to contractility in part in a "community"-dependent manner (Gurdon, 1988). Clearly, *isl* demonstrates the essential role of C-LTCC in the acquisition of normal cardiac form and function during embryonic development.

Results

isl Affects Heart Morphology and Function in Early Development

In wild-type zebrafish embryos, the heart first assembles from mesodermal precursors as a linear tube of two layers, the lining endocardium and the contractile myocardium (Stainier et al. 1996). The distinctive cell fate of the two heart chambers begins to diverge even prior to generation of the tube, but morphological distinction between the chambers becomes evident only after contractions begin. At that time, the ventricular myocardium begins to thicken both by concentric addition of myocardial cells as well as by enlargement (sometimes termed hypertrophy) of individual cells.

We isolated two alleles of the *island beat* (*isl*) mutation, isl^{m458} and isl^{m379}, as one of a group of mutations that perturb the onset of normal cardiac function from the

[3] Correspondence: fishman@cvrc.mgh.harvard.edu
[4] Present address: Jake Gittlen Cancer Research Institute, College of Medicine, Pennsylvania State University, 500 University Drive, Hershey, Pennsylvania 17033.

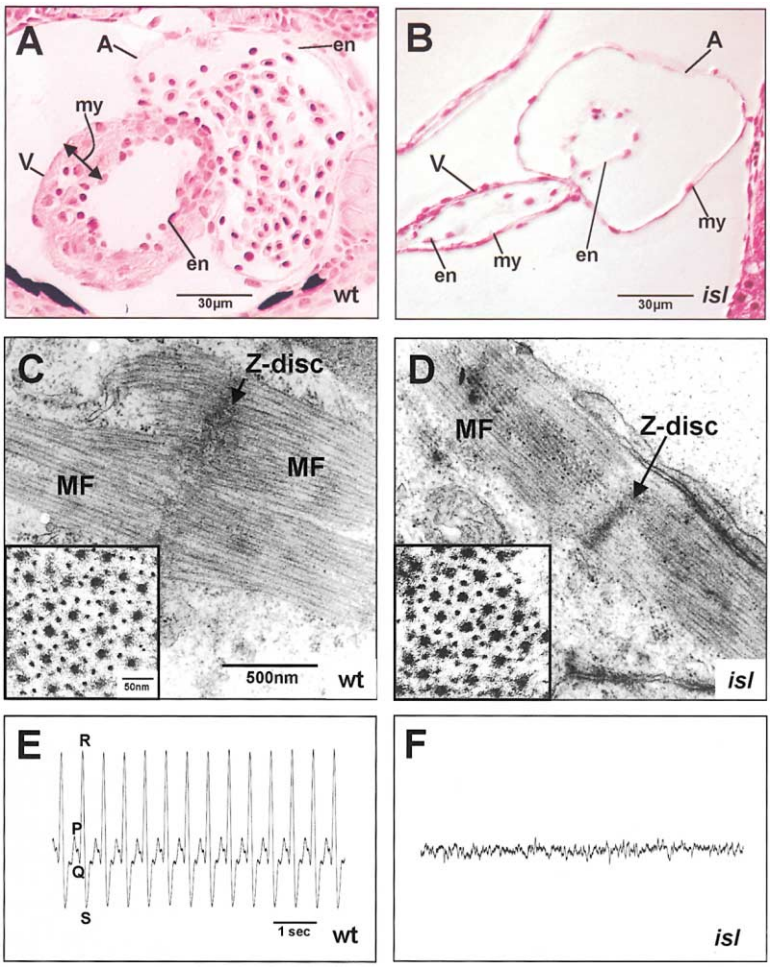

Figure 1. Effects of the *island beat* Mutation on Embryonic Heart Morphology and Electrical Activity

(A and B) Five micrometer sections of zebrafish embryonic hearts at 72 hpf. stained with hematoxylin/eosin.

(A) Normal histology of the heart in zebrafish embryos at 72 hpf. The myocardial wall has thickened in the ventricle (double-headed arrow). Nucleated blood cells are present in the atrium and the ventricle. A, atrium; V, ventricle; en, endocardium; my, myocardium.

(B) *isl* mutant embryos display a smaller ventricle with a single layer of myocardial (my) cells. Growth and hyperplasia of the ventricular wall is absent.

(C and D) Transmission electron microscopy of zebrafish embryonic hearts at 48 hpf. Myofibrillar arrays are evident, although relatively disorganized both in wild-type (C), and *isl* mutant (D) ventricles. Insets in (C) and (D) show higher magnifications of transverse sections of myofilaments. Thick and thin filaments are present both in wild-type and *isl* mutant.

(E and F) Electrocardiograms of wild-type and *isl* mutant embryos at 72 hpf.

(E) In wild-type embryos, the recording displays a small P wave, presumably derived from the atrium, preceding the QRS complex, representing ventricular electrical activity.

(F) In *isl* embryos, there is irregular electrical activity with small amplitude, presumably derived from the fibrillating *isl* atrium. QRS complexes are absent.

very first heart beat (Stainier et al., 1996). Both alleles are fully penetrant, and *isl*$^{m458/m379}$ transheterozygous embryos display the same phenotype as homozygotes for either single mutant allele.

isl mutant embryos form an apparently morphologically normal heart tube in anatomically correct position, containing both endocardium and myocardium. The first evident defect is an absence of the normal peristaltic contraction waves traversing the heart. Only cells in the future atrium of the heart tube contract, but do so in a sporadic and uncoordinated manner. *isl* mutants develop two chambers. However, the ventricular chamber is small and the ventricular myocardium remains single layered (Figures 1A and 1B). The atrial myocardium is a monolayer, as normal, and the overall size is not noticeably reduced. Contractions of ventricular myocytes are absent. In contrast, individual atrial cardiomyocytes do contract, but never in unison, in a pattern resembling atrial fibrillation. Impulse propagation to neighboring cells appears to be absent. A movie of *isl* heart function at 72 hr postfertilization (hpf.) is shown in supplemental material at http://www.developmentalcell.com/cgi/content/full/1/2/265/DC1. Aside from pericardial and yolk sac edema, *isl* embryos are not noticeably affected by the lack of normal blood flow during the first week of development.

Cardiac electrical activity, recorded with micropipettes placed in the vicinity of the heart, indicated that wild-type embryos (n = 20) shared the essential features of a normal electrocardiogram, including a smaller P wave, characteristic of atrial activity, preceding a larger QRS complex derived from the ventricle. In *isl* mutant embryos (n = 12), in contrast, no QRS complex was present, which is in agreement with ventricular silence, accompanied by low-amplitude rapid irregular activity as noted in atrial fibrillation (Figures 1E and 1F).

The *isl* Locus Encodes a Voltage-Gated L-Type Calcium Channel α1 Subunit

We performed mapping and positional cloning with the *isl*^{m458} allele. A genome-wide study of the segregation of microsatellite markers (Knapik et al., 1998) by bulked segregant analysis (Michelmore et al., 1991) linked *isl* to the marker Z9247 on linkage group 4. Genetic fine mapping placed the *isl* locus within a ~0.6 cM interval between the markers Z11657 and Z11566. We developed a physical map of this interval using YACs and BACs, as shown in Figure 2, and sequenced the two BACs 26g19 and 23c18 covering the *isl* interval.

Within the BACs coding sequence, only one gene, a zebrafish α1 subunit of the voltage-dependent L-type calcium channel, was identified (Figure 3). This gene

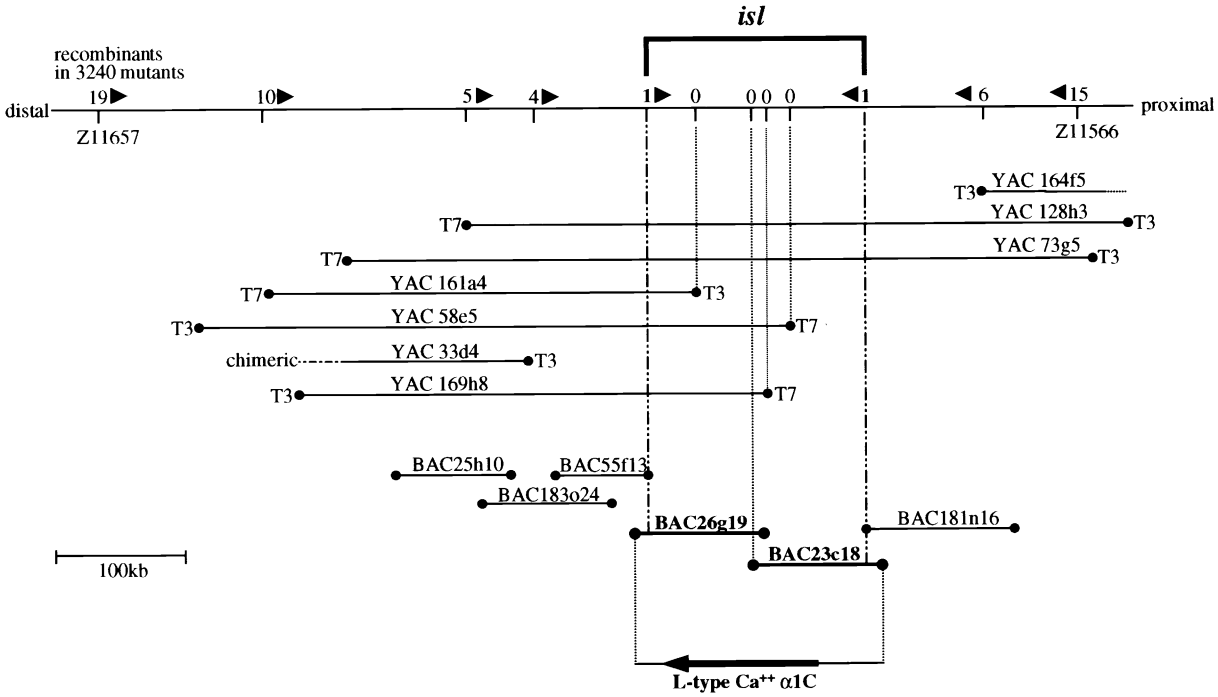

Figure 2. *isl* Encodes the Zebrafish α1C Subunit of the L-Type Calcium Channel

Integrated genetic and physical map of the zebrafish *island beat* (*isl*) region on linkage group 4. Genetic fine mapping placed the *isl* locus within a 0.6 cM interval between the markers Z11657 and Z11566. The number of recombinants between the tested markers and the *isl* locus are shown above the chromosome line. T7 ends from YACs 128h3 and 73g5 were used to isolate the four additional YAC clones 161a4, 58e5, 33d4, and 169h8. The BAC contig was assembled from six BACs using the different YAC ends as starting points. Subsequent testing of the BAC ends for recombination events narrowed the interval containing the *isl* gene to the BAC clones 26g19 and 23c18. The voltage-dependent L-type calcium channel α1C subunit was the only gene identified in this interval.

extends over ~150,000 bp of genomic DNA. Conceptual translation of genomic DNA and cDNA sequences (GenBank accession number AF305689) revealed a high degree of homology (78% amino acid identity) to the α1C subunit of the human voltage-dependent L-type calcium channel (C-LTCC_h; Figure 3C). The overall structure of the zebrafish C-LTCC (C-LTCC_z) seems to be identical to previously described α1 subunits of LTCCs, and consists of four domains (I–IV) each containing six transmembrane segments (S1–S6), including a positively charged and highly conserved S4 segment (100% conserved, compared to human C-LTCC; Figure 3A). Less-conserved regions include the cytoplasmic loop between domains II and III, and the distal part of the carboxyl terminus. Conserved synteny between human and zebrafish was observed in the region of the C-LTCC gene, namely zebrafish linkage group 4 and human chromosome 12, in further agreement with the notion that *isl* is the zebrafish ortholog of the human C-LTCC.

Mutations in the *isl* Alleles Lead to Truncation in the Pore-Forming Transmembrane Domains III and IV of the L-Type Calcium Channel α1 Subunit

To identify the site of the ENU-induced mutations, we sequenced the entire zebrafish coding sequence of C-LTCC from wild-type and from the two different *isl* alleles. The *isl*^{m458} allele has a C-to-T nucleotide transversion at the first base of codon 1077 (CAG → TAG). This would predict a change of a glutamine to a stop codon (Q1077X), causing premature termination of translation prior to the transmembrane segment S6 of domain III (Figures 3A and 3B). The *isl*^{m379} allele has a T-to-A nucleotide transversion in codon 1352 (TTG → TAG). This would predict a change of a leucine to a stop codon (L1352X), and would cause premature termination of translation prior to the pore-forming transmembrane segment S5 of domain IV (Figures 3A and 3B). Therefore, as outlined in Figure 3A, both mutations would lead to the truncation of C-LTCC in different domains, either in the pore-forming region of domain III (*isl*^{m458}) or domain IV (*isl*^{m379}), respectively.

isl mRNA Is Expressed in Cardiac Precursors, the Heart, and the Pancreas in Early Zebrafish Development

By RNA in situ hybridization, C-LTCC expression is first evident at the 21-somite stage, in the cardiac precursors of the lateral plate mesoderm (Figures 4A and 4B). By 26 hpf., C-LTCC expression is restricted to the heart tube and the pancreatic primordium (Figures 4C and 4D). At 48 hpf., additional expression in the gut tube and the central nervous system begins. C-LTCC expression level and location does not differ between wild-type and *isl* mutant embryos. To our knowledge, there is no systematic study of the expression pattern of the LTCC α1C subunits in vertebrates, but the zebrafish C-LTCC expression pattern is similar to that observed in other vertebrates (Iwashima et al., 1993; Takimoto et al., 1997).

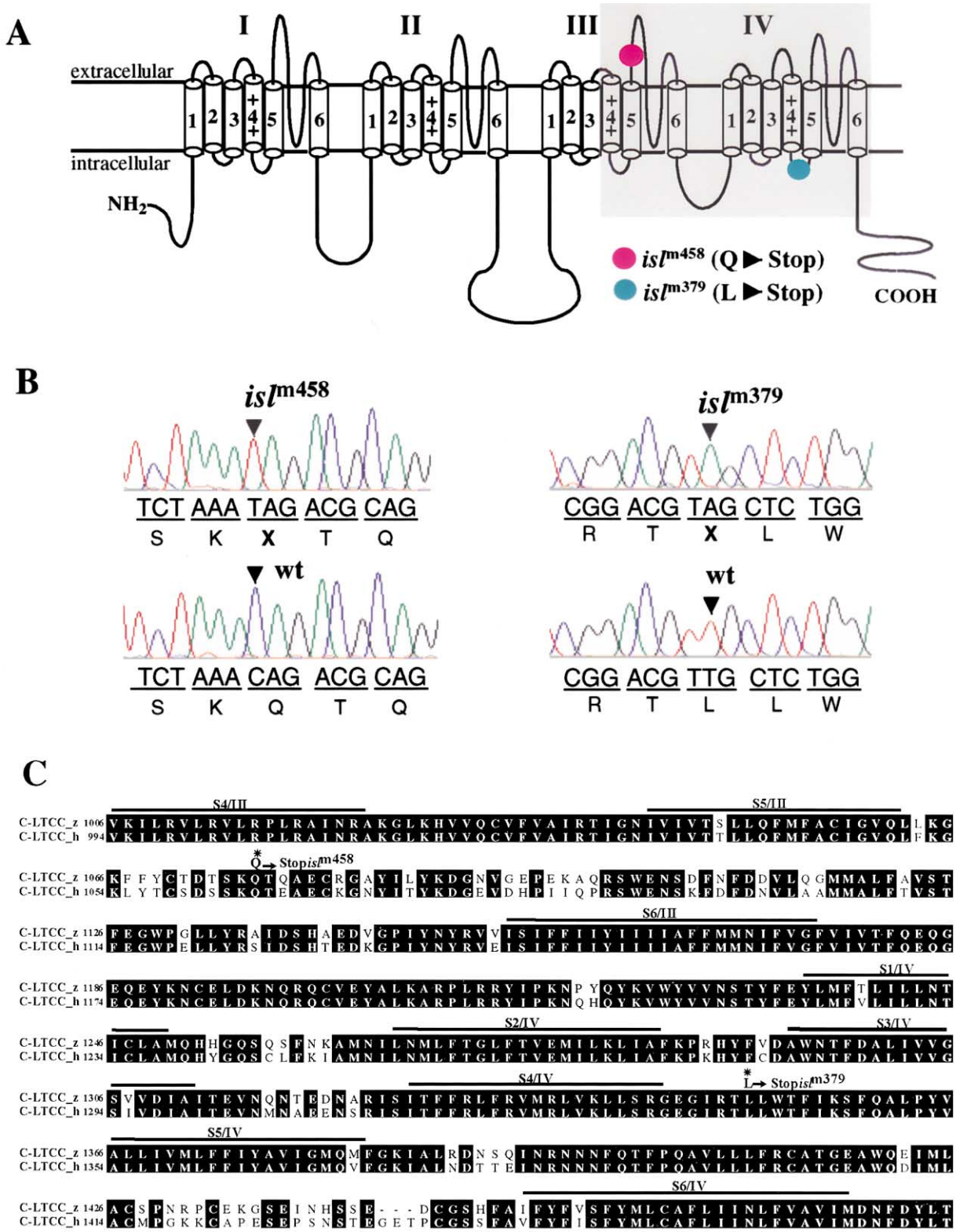

Figure 3. Mutations in *isl* Lead to Premature Termination of Translation of the Highly Conserved C-LTCC

Domain structure of the zebrafish C-LTCC, partial sequence alignment of zebrafish and human C-LTCC proteins, and position of the *isl* mutations.

(A) Diagram of the zebrafish voltage-gated calcium channel α1 subunit, containing four repeat domains (I–IV). Each repeat domain contains six transmembrane segments (S1–S6). The amphipathic transmembrane segment (S4) is indicated by a plus sign. The location of the *isl* mutations (*isl*^{m458} and *isl*^{m379}) are depicted by colored circles and the predicted amino acid changes are displayed. Both mutations are predicted

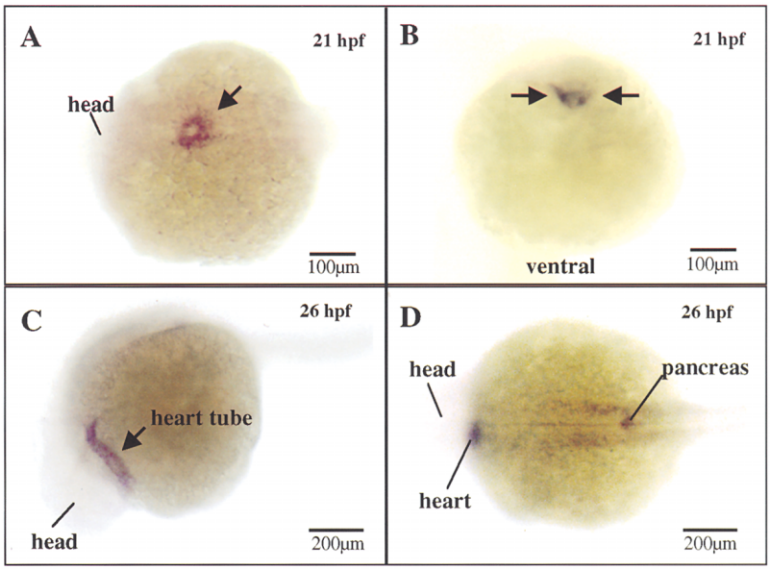

Figure 4. C-LTCC (*isl*) RNA Expression in Cardiac Precursors, the Heart Tube, and the Pancreas in Early Zebrafish Development

(A and B) C-LTCC (*isl*) RNA expression in 24-somite zebrafish embryos is limited to the bilateral cardiac precursors. Dorsal view (A); frontal view (B).

(C and D) By 26 hpf., C-LTCC expression is restricted to the heart tube. Lateral view (C) and dorsal view (D), showing additional expression in the pancreatic primordium.

isl Mutations Abolish L-Type Calcium Currents in Cardiomyocytes

Since the protein truncations in the alleles *isl*^{m458} and *isl*^{m379} are expected to have dramatic effects on C-LTCC function, we examined the functional consequences of the mutations on the L-type calcium currents of *isl* cardiocytes. The whole-cell voltage-clamping technique was applied to *isl* embryonic cardiocytes isolated and briefly cultured from 72 hpf. embryonic hearts. The diminutive size of the embryonic zebrafish heart (100–150 μm) precluded separation of atrium from ventricle.

To prevent calcium-induced inactivation of LTCCs, we recorded currents in calcium-free solution with barium (Ba^{2+}) as the charge carrier. LTCCs-mediated Ba^{2+} currents were evident as inward currents that appeared by membrane depolarization from a holding voltage of −60 mV to voltages more positive than −30 mV. With Ba^{2+} as the charge carrier, the currents decreased only slowly over time (Figure 5). To maximize the separation of L- and T-type calcium currents, we took advantage of their different responses to voltage. T-type currents were largest when the cell membrane was held at −100 mV and the test voltage was −30 mV. L-type currents were prominent when the cells were held at a depolarized voltage of −60 mV to inactivate the T-type channels. The maximum L-type currents were then elicited by stepping the membrane to −10 mV (Figure 5). All wild-type zebrafish embryo cardiomyocytes tested (n = 14) expressed both T- and L-type Ba^{2+} currents, which were sensitive to either nickel or nifedipine (Baker et al., 1997). In *isl*^{m458} cardiomyocytes (n = 13), however, L-type Ba^{2+} currents were greatly reduced or absent. T-type Ba^{2+} currents, in contrast, were present in *isl* cells (n = 13; Figure 5). Holding the cells at −100 mV and depolarizing to −10 mV showed that the average inward current obtained after 400 ms was dramatically reduced in *isl*^{m458} cells (n = 13; −3.5 pA ± 0.69 pA SEM) in comparison to wild-type cells (n = 14; −20.95 pA ± 6.43 pA SEM; $p < 0.03$). Similar results were obtained with a holding voltage of −60 mV. Mean cell capacitances were the same for wild-type and mutant cells (2.5–2.8 pF).

Lack of Heart Growth without Evident Subcellular Defects in the Cardiocytes of *isl* Mutants

The most evident morphological defect in the *isl* embryo is the small size of the ventricle (Figures 1A and 1B). At about 60 hpf. of embryonic development, the ventricle normally gets larger by apposition of individual cardiocytes. The consequence is a thickening of the ventricular wall as well as growth along the long axis of the heart. We found, by examination of serial sections of zebrafish embryonic hearts at 72 hpf., a reduced number of myocardial cells in the ventricle of *isl* versus wild-type hearts (*isl*: 200 ± 22, n = 6; wild-type 350 ± 38, n = 6, mean ± SEM). This appears to be a consequence of the loss of

to truncate C-LTCC at the indicated locations. Amino acid sequence comparison of the zebrafish and human C-LTCC from the shaded area is displayed in (C).

(B) Point mutations in the two different alleles *isl*^{m458} and *isl*^{m379} lead to the creation of a premature stop codon. The *isl*^{m458} allele has a C-to-T nucleotide transversion at the first base of codon 1077 (CAG → TAG) predicting a change from glutamine to a stop codon (Q1077X). The *isl*^{m379} allele has a T-to-A nucleotide transversion in codon 1352 (TTG → TAG), predicting a change from leucine to a stop codon (L1352X). Amino acid translation derived from the codons is shown below the base pair readouts. The mutated base pairs are marked with arrows. wt, wild-type.

(C) Partial amino acid sequence alignment of the zebrafish (C-LTCC_z) and the human (C-LTCC_h) voltage-dependent L-type calcium channel α1C subunit from transmembrane domains III-S4 to IV-S6. Domains and segments are indicated above the alignment. Black boxes: amino acid identity. *isl* mutation sites are indicated by asterisks. There is 100% amino acid identity between C-LTCC_z and C-LTCC_h in the S4 segments, high homology in the transmembrane segments S1, S2, S5, and S6, but less homology especially in the extracellular regions between S5 and S6. The GenBank accession numbers for C-LTCC_h and C-LTCC_z are AJ224873 and AF305689, respectively.

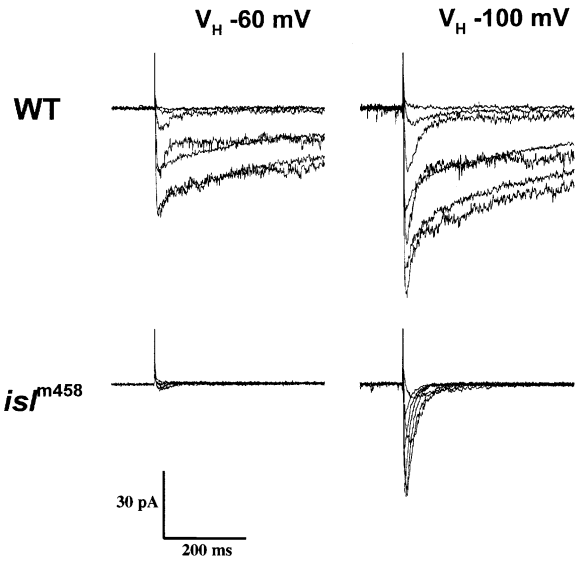

Figure 5. Absence of L-Type Ba^{2+} Currents in *isl*^{m458} Cardiocytes

Currents were recorded in calcium-free solutions with Ba^{2+} as a charge carrier to prevent calcium-induced inactivation of the L-type calcium channel. Representative experiments are shown for the wild-type (n = 13) and *isl* mutant cardiocytes (n = 13). Representative currents were obtained by holding the cell membrane at either −60 mV (V_H −60 mV) or −100 mV (V_H −100 mV) and depolarizing the membrane in 10 mV steps between −50 mV and +10 mV.

calcium signaling rather than secondary to the contractility failure of the *isl* ventricle. The phenotype of the zebrafish *tell tale heart* (*tel*) mutation is nearly identical to *isl* (Stainier et al., 1996). The ventricle is silent and there is no blood flow. There is slight twitching of the atrium in the vicinity of the atrio-ventricular junction (see supplemental movies). *tel* encodes a myofibrillar gene (W.R. and M.C.F., unpublished data). However, the number of ventricular cells is not reduced in *tell tale heart* (342 ± 32, n = 6, mean ± SEM). In addition, there is no evident apoptosis of myocardial cells in either wild-type or *isl* hearts at this stage, as revealed by terminal deoxynucleotide transferase-mediated dUTP-biotin nick end-labeling (TUNEL; Gavrieli et al., 1992).

Ineffective calcium entry might perturb growth at several levels. In particular, calcium is known to be important to the regulation of transcriptional activity of many genes, including myocyte enhancer factor 2C (MEF2-C; Black and Olson, 1998). However, we find in *isl* mutant hearts by RNA in situ hybridization no detectable changes in myocardial expression levels of genes that regulate early cardiac cell fate decisions, including the homeodomain transcription factor Nkx2.5, the MADS box transcription factor MEF2C, or the basic helix-loop-helix factor dHAND (Carrion et al., 1999; Mellstrom and Naranjo, 2001; van Haasteren et al., 1999) at any developmental stage examined (18 somites, 21 somites, 24 hpf., 36 hpf., and 48 hpf. and data not shown).

LTCC-mediated calcium uptake might also regulate, by control of transcriptional activity of MEF2C, the expression of downstream genes responsible for the synthesis of myofibrils. However, mRNA levels for myosin light chain 1, myosin light chain 2a, ventricular myosin heavy chain, α-tropomyosin, and desmin displayed a normal temporal, spatial, and quantitative distribution in *isl* mutant embryos during the first 48 hr of development (data not shown).

At an ultrastructural level, there are no obvious differences between wild-type and mutant myocardial cells. As shown in Figures 1C and 1D, myofibrillar arrays are evident in both wild-type and *isl* myocardium at 48 hpf. Subtle quantitative differences might be indiscernible, however, given the lack of higher order sarcomeric structures at this stage of development. The morphologies of mitochondria and cell-cell junctions (gap junctions, zonae adherentes, and desmosomes) are also not noticeably different between wild-type and *isl* embryos.

isl Ventricular Cardiocytes Are Unresponsive to Electrical Stimulation

Since LTCC current is required for atrio-ventricular conduction, failure of conduction from the normal pacemaking site in the atrium could lead to ventricular silence in *isl.* Therefore, we examined excitability and conduction by direct electrical stimulation of the heart chambers. Stimulation of the wild-type atrium (n = 20) drove contractions of the chamber at rates up to 220 impulses/min, in all cases followed by ventricular contraction, at a 1:1 ratio. Direct stimulation of the wild-type ventricle (n = 20) led to coordinated contraction of the ventricular chamber, without retrograde impulse propagation to the atrium. No sites in either chamber were refractory to such pacing.

In contrast, stimulation of *isl* atria (n = 20) elicited only localized contractions of atrial cells in the immediate vicinity of the electrode, which were never propagated to either the adjacent atrial wall or the ventricle. Hence, there clearly is no conduction from atrium to ventricle. In agreement, we found that verapamil blockade of LTCCs similarly prevents atrio-ventricular conduction in wild-type zebrafish embryos (data not shown). However, direct stimulation of *isl* ventricles (n = 20) does not evoke contraction even of the ventricular myocytes touched with the microelectrode. Hence, although failure to conduct from the atrium may partially account for ventricular silence, it seemed as though the most proximate cause is inexcitability or electromechanical uncoupling of the *isl* ventricular cells.

Transplanted Wild-Type Cell Clusters Contract in *isl* Ventricles

The inexcitability of the *isl* ventricle presumably reflects the requirement for calcium entry to engage the contractile apparatus at the single-cell level. However, there is evidence that certain attributes of cell development in the embryo are coordinated at multicellular levels (Gurdon et al., 1993). To ensure cardiac cell contractility, in particular, it is crucial that mechanical and electrical activity is relatively uniform throughout a chamber (DeMello, 1994). To examine this, we studied the behavior of wild-type cells in the hearts of *isl* mutant embryos. Reciprocal transplantation of *isl* cells into wild-type hearts was uninformative, because the vigorous contraction of wild-type cells makes reliable ascertainment of whether a transplanted *isl* cell is truly immobile infeasible. We performed transplantations at the blastula

Table 1. Transplantation of Wild-Type Single Cells or Cell Clusters into *isl* Myocardium

		Transplants	Contracting Transplants
Atrium	single cell	42	42
	cell cluster	5	5
Ventricle	single cell	48	0
	cell cluster	10	10

Summary of the results of the transplantation of wild-type cells into *isl* myocardium. Transplanted embryos were scored by video microscopy for contraction of the transplanted fluorescent cells. The locations of the transplanted cells in the *isl* hearts were confirmed by staining and sectioning. The beating cell clusters of wild-type cells observed contained at least three myocardial cells in contiguity.

stage and then evaluated the contractility of the labeled transplanted cells once the heart had developed.

We found that single wild-type cells transplanted in *isl* atria (n = 42) contract. These wild-type cells did not drive contraction of the surrounding *isl* mutant cardiocytes, which continued their own episodic sporadic contractions independently of each other. Therefore, the contractile phenotype is cell autonomous in the atrium (Table 1).

Single wild-type cells in *isl* ventricles (Figures 6A and 6B), however, did not contract (n = 48). This suggests that there is a cell-nonautonomous element to contractile failure in the *isl* ventricle as opposed to the *isl* atrium. To examine this, we progressively increased the transplant load to generate small wild-type cardiocyte clusters (n = 10) in *isl* ventricular myocardium, of a size shown in Figures 6C and 6D. Labeled wild-type cells under these conditions clearly beat, although they never rescue contraction in neighboring cardiocytes around the border of the transplanted cluster (Table 1). This suggests that maturation of the contractile phenotype in the embryonic ventricle is coordinated among cells in a manner in part dependent on C-LTCC function.

Discussion

Zebrafish *island beat* Embryos Contain Loss-of-Function Mutations in the α1C Subunit of the L-Type Calcium Channel

Here, we show that the *isl* locus contains a mutated form of the zebrafish voltage-dependent LTCC α1C subunit. We find that this channel is essential for normal embryonic heart function and morphogenesis, with distinctive requirements in ventricular and atrial chambers.

LTCCs are heteromeric proteins consisting of an α1 subunit with accessory α2/δ and β subunits. The α1 subunit includes the voltage sensor, the ion selectivity pore, and drug binding sites for dihydropyridines (Catterall, 1995). This subunit consists of four transmembrane domains (I–IV), each consisting of six transmembrane segments (S1–S6; Lehmann-Horn and Jurkat-Rott, 1999). Cytosolic N and C termini of the α1 subunit are thought to be critical for channel gating (Shistik et al., 1999; Zuhlke et al., 1999). The two mutations reported here truncate the protein prior to S6 of domain III (*isl*^{m458}) or S5 of domain IV (*isl*^{m379}), by analogy predicted to abrogate or markedly reduce channel function. Whole-cell patch clamp analysis confirmed the absence of L-type calcium

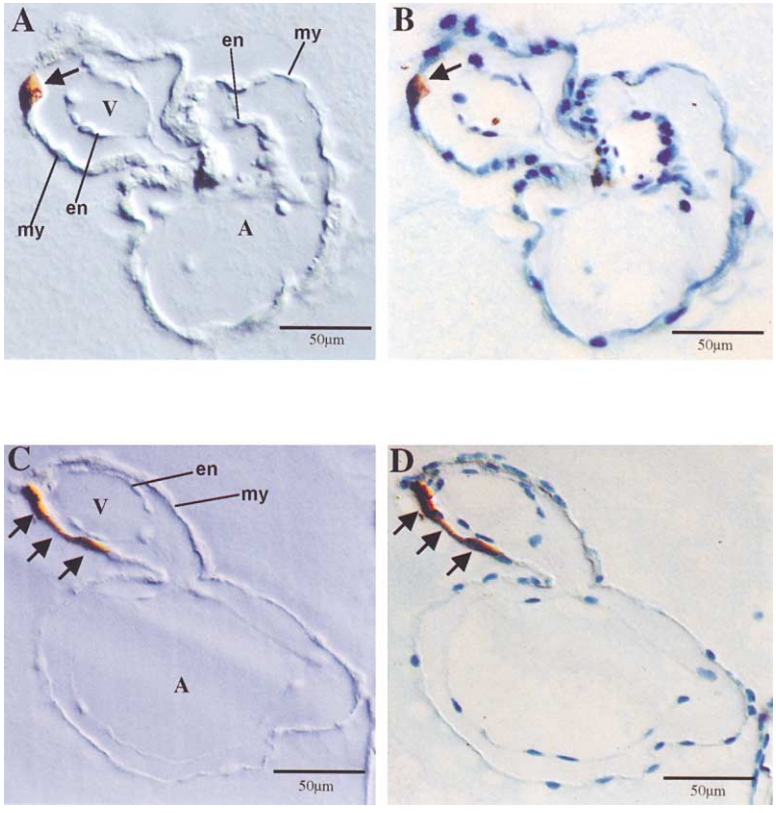

Figure 6. Integration of Labeled, Transplanted Wild-Type Cells into the *isl* Myocardial Layer of the Ventricle (*isl*/Wild-Type Heart Chimera)

(A) Single labeled noncontractile wild-type cell (arrow) in *isl* ventricle.

(B) Counterstaining of the same section with methylene blue-azure II to display cell nuclei and endocardial and myocardial layers.

(C) A contracting cluster of wild-type cells (arrows) transplanted into the *isl* myocardial layer of the ventricle.

(D) Counterstaining of the same section with methylene blue-azure II. V, ventricle; A, atrium; en, endocardium; my, myocardium.

currents, with maintenance of T-type calcium currents in *isl* cardiocytes.

C-LTCC Is Required for Ventricular Growth and Contractility in Embryonic Development

It was not anticipated that the ventricle of *isl* mutant embryos would grow so poorly. As demonstrated here, this is not explained as a consequence of silence, because other zebrafish mutations, such as *tell tale heart* can cause silence of the ventricle without similar growth deficiencies.

Although little is known about the molecular pathways linked to cardiac growth during embryonic development, a critical role for calcium in signal transduction begins to evolve (MacLellan and Schneider, 2000; Frey et al., 2000). For instance, overexpression of a calcineurin transgene in the heart of mice induced cardiac hypertrophy (Molkentin et al., 1998). It has even been proposed that calcium-dependent pathways serve as the unifying mechanism by which human mutations in myofibrillar genes lead to hypertrophy (Seidman and Seidman, 2001). With regard to these proposals, therefore, it might not be surprising that abrogation of LTCC activity diminishes normal cardiac growth during embryogenesis.

The inability of *isl* ventricular cells to contract is unlikely to be due to poor growth per se, because the *isl* cells do synthesize myofibrillar proteins and assemble them into normal-appearing sarcomeres. It is likely, therefore, that ventricular silence in *isl* embryos reflects to a large degree the dependence of the cells on extracellular calcium for the triggering of contraction, especially before maturation of the sarcoplasmic reticulum (Brotto and Creazzo, 1996; Fabiato, 1982). Similarly, skeletal muscle contractions are absent in autosomal recessive lethal murine muscular dysgenesis, which is caused by a nonsense mutation in the skeletal muscle α1S subunit of the LTCC (Chaudhari, 1992). Skeletal and cardiac muscle, of course, differ in handling and dependence upon calcium (Tanabe et al., 1988). However, both cardiac ventricular and skeletal muscles are rendered noncontractile when their LTCCs are absent during all of development. Surprisingly, targeted mutation of C-LTCC in mice embryos did not interfere with early embryonic heart contractility and morphology, although the mice died in later embryogenesis of undefined cause (Seisenberger et al., 2000). However, in contrast to *isl* zebrafish embryos, cardiocytes of homozygous mutant mice retained L-type currents of unidentified source, probably accounting for the phenotypic difference.

Since LTCC currents are required for atrio-ventricular conduction, failure of conduction from the normal pacemaking site in the atrium could also lead to ventricular silence in *isl.* However, this is not the critical cause of the contractile failure, because clusters of wild-type cells can generate spontaneous contractions in the midst of an *isl* ventricle. In addition, wild-type cardiocytes appear to be rendered noncontractile by contact with other *isl* cells. A single wild-type cell does not contract in an *isl* ventricle, although it does in an *isl* atrium. Since the atrium and ventricle in the mutant both are single layered and thin, there is no obvious mechanical reason to explain this deficiency. Rather, the fact that several wild-type cells in contiguity contract in the *isl* ventricle suggests that cell interactions among the cardiocytes may help to regulate each other's differentiation. There are other examples in development when a cell's fate needs to be closely coordinated with those of its neighbors. One type of neighbor-dependent differentiation, termed the "community effect" (reviewed in Gurdon et al., 1993), is revealed by transplantation, such that progenitor cells transplanted ectopically complete differentiation as either muscle (Gurdon, 1988) or nerve (Galli et al., 2000) only in clusters, not as single cells. Cells can even have their fate completely changed, as described by Mangold, a process termed homoiogenetic induction (Mangold, 1933). The mechanisms of such effects are not known, although presumed to include signaling cascades initiated through cell surface receptors or gap junctions (Gurdon et al., 1993). Our results indicate that maturation of the contractile phenotype in the embryonic ventricle is coordinated among cells in a "community"-dependent manner, in part relying upon C-LTCC function.

Atrial Cells Contract in an Uncoordinated Fashion in the Absence of *isl*

Atrial cardiocytes do contract in *isl* embryos, both spontaneously and in response to electrical stimulation. However, since atrial and ventricular cardiocytes develop along different molecular pathways (Nguyen-Tran et al., 1999), it is not surprising that their response to the same mutation may be distinctive.

The fact that the atrial cells do contract indicates the presence of an alternative source of calcium to *isl* atrial cells. Since we cannot confidently separate and record from atrial versus ventricular cells, it is conceivable that alternative L-type currents in the atrium, such as those mediated by α1D subunits of the LTCC (D-LTCC), which are expressed in mammalian atrial cells and known to modulate sinoatrial activity (Platzer et al., 2000), may affect this mechanism. However, *isl* atrial activity in vivo could not be suppressed by dihydropyridine receptor blockade, which is known to be effective on all types of LTCCs, including D-LTCCs. Another calcium source to *isl* atrial cells could be derived from the T-type calcium currents, which are preserved in *isl* cardiocytes. Along these lines, it is interesting that the scattered atrial contractions in the atrium of *isl* mutant embryos resemble those of the common human disorder atrial fibrillation, a disorder associated with diminution of L-type and retention of T-type calcium currents in human biopsy tissue (reviewed in Nattel and Li, 2000). Alternatively, as in embryonic stem cells undergoing early cardiogenic differentiation, there might be fluctuations in intracellular calcium from developing intracellular stores (Viatchenko-Karpinski et al., 1999), accounting for the *isl* atrial phenotype.

Cardiac Function in Vertebrate Embryos

Most molecular embryology has been concerned with generation of embryonic form. Far less attention has been paid to the choreographing of physiological functions in the embryo. The transparency of zebrafish embryos facilitates the assessment of embryonic cardiac

function by light microscopy, with confirmation and quantitation possible by direct hemodynamic measurements. For the study of vertebrate cardiovascular development, zebrafish embryos have, in comparison to mammals, the advantage that they depend upon diffusion from the environment rather than circulatory delivery of oxygen to maintain metabolism and prevent hypoxia (Pelster and Burggren, 1996). Thus, using mutagenized zebrafish, we are able to identify mutants with cardiac defects, analyze their effects on embryonic cardiac function in the intact animal, study the cellular defect, define cell autonomy of the gene's function, and finally, identify the mutated gene by positional cloning, confident that the functional defect directly reflects a primary role of the gene in vivo in the embryo, unencumbered by complications of hypoxia. This ability to complement genetics with both organismic and cellular physiology makes the zebrafish particularly powerful for cardiovascular functional genomics.

Experimental Procedures

Zebrafish Strains and Studies

Care and breeding of zebrafish *Danio rerio* was as described (Westerfield, 1995). Developmental staging was carried out using standard morphological features (Kimmel et al., 1995) of fish raised at 28.5°C.

Electrocardiograms and Electrical Stimulation

Embryos were anesthetized with 3-aminobenzoic acid ethyl ester to inhibit skeletal muscle movements. For recording of cardiac electrical activity, patch clamp pipettes (2–5 MΩ) were approached to the heart and tail regions of the embryo. Voltage signals were recorded in the current mode configuration with a Dagan 3900 amplifier (Dagan), and filtered with an eight-pole Bessel filter (Frequency Devices).

After dissecting the pericardial sac of wild-type and *isl* mutant embryos (72 hpf.), electrical stimulation was performed using a pulsar digital stimulator IS-PL-06 (FHC). Patch clamp pipettes with an impedance of 2–5 MΩ were used as probes and approached to either the atrium or ventricle with a micromanipulator under microscopic control. Different areas of the atrial and ventricular wall were touched with the electrode. No differences were observed in the contractile response. The heart chambers were stimulated at different rates (100–220/min), applying 0.001–0.01 mA currents (pulse duration, 73 μsec).

Transmission Electron Microscopy

Embryos were fixed as described in Majumdar and Drummond (1999), embedded in Epon 812 (Polysciences), and sectioned. Thin sections were cut on a Reichert Ultracut E ultramicrotome and collected onto Formar-coated slot grids. Sections were poststained with uranyl acetate and lead citrate and viewed in a Philips CM10 electron microscope at 80 keV.

Genetic Mapping and Positional Cloning

DNA from 24 mutant and 24 wild-type *isl*^{m458} embryos was pooled for bulked segregation analysis (Michelmore et al., 1991). One hundred and twenty microsatellite markers from the zebrafish genetic map (Knapik et al., 1998) were tested for possible linkage.

The critical genomic interval for *isl* was defined by genotyping 3240 mutant *isl*^{m458} embryos for microsatellite markers in the area. YAC clones around Z11566 were isolated from PCRable DNA pools (Research Genetics), and ends were rescued by self-circularization (Zhong et al., 1998). A second generation of YAC clones (161a4, 58e5, 33d4, and 169h8) was isolated using the T7 ends of YAC 128h3 and 73g5. The BAC contig was assembled using the proper YAC ends as starting points. The length of all BAC clones was determined by pulsed-field gel electrophoresis (PFGE). Recombinant fine mapping analysis was performed with single-stranded conformation polymorphisms (SSCP) from the sequence of rescued YAC and BAC ends.

Construction of Genomic DNA Shotgun Libraries and Sequence Assembly

Genomic DNA shotgun libraries of BAC 23c18 and BAC 26g19 were made by shearing DNA with a Sonic cup-horn dismembrator (model 550, Fisher Scientific) and digesting the DNA with mung bean nuclease (New England Biolabs). The DNA was then size selected on agarose gels (1500–4000 bp) and blunt end-ligated into pUC 19 (New England Biolabs). High-throughput plasmid DNA preparations were performed with the Robot 9600 (Qiagen). Shutgun sequencing was carried out with an ABI 377 sequencing system (Perkin Elmer). Sequence tracings were read and processed by the Phred program. pUC19 sequence was clipped off using CrossMatch. Eighteen interconnected sequence contigs were assembled using Phrap and edited by Consed (http://www.phrap.org/).

Sequence Comparison and Mutation Detection

Contigs generated by the Phred/Phrap software package were compared to known sequences using the basic local alignment search tool (BLAST 2.0) from the National Center for Biotechnological Information (http://www.ncbi.nlm.nih.gov/blast/). Program blastx was applied to screen the nr database.

The cDNA sequence for the zebrafish α1C subunit of the L-type (C-LTCC) was determined by reverse transcriptase polymerase reaction (RT-PCR) and rapid amplification of cDNA ends (RACE; Clontech) and deposited at GenBank (accession number AF305689). RNA from mutant and wild-type whole embryos or dissected embryonic hearts was isolated using TRIZOL Reagent (Life Technologies). The oligonucleotide sequence was based on information from the genomic sequence contigs. PCR products were cloned with the TOPO TA cloning kit (Invitrogen). Four independent clones were sequenced for each cloned fragment. For the alleles *isl*^{m458} and *isl*^{m379}, genomic DNA from mutant, heterozygote, and homozygote embryos was amplified around the point mutations, cloned, and sequenced to confirm the mutations detected.

In Situ Hybridization

Whole-mount RNA in situ hybridization was carried out as described (Jowett and Lettice, 1994). A 1224-bp fragment of cDNA that contains exon 17 through 28 of the zebrafish α1C subunit of the LTCC was subcloned in pCR II (Invitrogen) for in vitro transcription (Boehringer). RNA probes were digoxygenin labeled (Boehringer).

Patch Clamp Recordings

Hearts from tricaine-anesthetized day 3 mutant embryos were removed and cells prepared as described (Baker et al., 1997). Cardiomyocytes from the wild-type line AB were used as controls. Standard whole-cell recordings (Hamill et al., 1981) were performed at room temperature (21°C–23°C), essentially as described (Baker et al., 1997). All data were acquired and analyzed blind to the genotype. Currents were recorded in calcium-free solutions with Ba^{2+} as the charge carrier to prevent calcium-induced inactivation of the L-type calcium channel. The bath solution contained $BaCl_2$ (15 mM), CsCl (5 mM), HEPES (10 mM), glucose (10 mM), and N-methyl-D-glucamine (125 mM) (pH 7.4 with HCl). Pipette solution contained tetraethylammonium chloride (140 mM), $MgCl_2$ (0.5 mM), HEPES (10 mM), EGTA (10 mM), MgATP (5 mM), and cAMP (0.1 mM) (pH 7.4 with CsOH). Pipettes were fire polished to resistances of 2–5 MΩ. Current traces were filtered at 1 kHz. Linear leak currents were determined by a small depolarizing step, and subtracted from all subsequent records. Data acquisition and analysis were carried out using pClamp6 software (Axon Instruments).

Transplantation

Embryos used for transplantation experiments were produced by intercrossing *isl*$^{m458/+}$ fish, thus yielding a wild-type to mutant embryo ratio of 3:1. 3% tetramethylrhodamine dextran and 3% biotin dextran (Molecular Probes) were mixed in 0.2 M KCl and pressure injected into wild-type donor embryos (AB) at the 1- to 2-cell stage. Labeled

donor cells from the margin were transplanted at early blastula stage to the margins of *isl* embryos using methodology described by Lee et al. (1994). After 24, 48, and 72 hr of development at 28.5°C, embryos were inspected with fluorescence microscopy and movies of beating cells were recorded. To inhibit pigmentation, 0.003% 1-phenyl-2-thiourea was added to the embryo medium at 24 hpf. To confirm the integration of labeled wild-type cells into *isl* ventricular or atrial myocardial layers, whole embryos were stained with anti-biotin antibodies (DAB), fixed with 4% paraformaldehyde, embedded in JB4, and sectioned in transverse or sagittal orientation.

Acknowledgments

We thank M.H. Boulos and M. McKee for excellent technical assistance. This work was supported by grants from NIH (5R01HL49579, 5R01DK55383, and 1RO1HL63206 [M.C.F.]), Deutsche Forschungsgemeinschaft Ro 2173/1-1 (W.R.), and a New Investigator Grant from the Foundation for Anesthesia Education and Research and the Society for Cardiovascular Anesthesiologists (K.B.).

Received March 19, 2001; revised May 7, 2001.

References

Baker, K., Warren, K.S., Yellen, G., and Fishman, M.C. (1997). Defective "pacemaker" current (Ih) in a zebrafish mutant with a slow heart rate. Proc. Natl. Acad. Sci. USA *94*, 4554–4559.

Black, B.L., and Olson, E.N. (1998). Transcriptional control of muscle development by myocyte enhancer factor-2 (MEF2) proteins. Annu. Rev. Cell Dev. Biol. *14*, 167–196.

Brotto, M.A., and Creazzo, T.L. (1996). Ca2+ transients in embryonic chick heart: contributions from Ca2+ channels and the sarcoplasmic reticulum. Am. J. Physiol. *270*, H518–H525.

Carrion, A.M., Link, W.A., Ledo, F., Mellstrom, B., and Naranjo, J.R. (1999). DREAM is a Ca2+-regulated transcriptional repressor. Nature *398*, 80–84.

Catterall, W.A. (1995). Structure and function of voltage-gated ion channels. Annu. Rev. Biochem. *64*, 493–531.

Chaudhari, N. (1992). A single nucleotide deletion in the skeletal muscle-specific calcium channel transcript of muscular dysgenesis (mdg) mice. J. Biol. Chem. *267*, 25636–25639.

DeMello, W.C. (1994). Gap junctional communication in excitable tissues; the heart as a paradigm. Prog. Biophys. Mol. Biol. *61*, 1–35.

Fabiato, A. (1982). Calcium release in skinned cardiac cells: variations with species, tissues, and development. Fed. Proc. *41*, 2238–2244.

Frey, N., McKinsey, T.A., and Olson, E.N. (2000). Decoding calcium signals involved in cardiac growth and function. Nat. Med. *6*, 1221–1227.

Galli, R., Borello, U., Gritti, A., Minasi, M.G., Bjornson, C., Coletta, M., Mora, M., De Angelis, M.G., Fiocco, R., Cossu, G., and Vescovi, A.L. (2000). Skeletal myogenic potential of human and mouse neural stem cells. Nat. Neurosci. *3*, 986–991.

Gavrieli, Y., Sherman, Y., and Ben-Sasson, S.A. (1992). Identification of programmed cell death in situ via specific labeling of nuclear DNA fragmentation. J. Cell Biol. *119*, 493–501.

Gurdon, J.B. (1988). A community effect in animal development. Nature *336*, 772–774.

Gurdon, J.B., Lemaire, P., and Kato, K. (1993). Community effects and related phenomena in development. Cell *75*, 831–834.

Hamill, O.P., Marty, A., Neher, E., Sakmann, B., and Sigworth, F.J. (1981). Improved patch-clamp techniques for high-resolution current recording from cells and cell-free membrane patches. Pflugers Arch. *391*, 85–100.

Hermsmeyer, K., Mishra, S., Miyagawa, K., and Minshall, R. (1997). Physiologic and pathophysiologic relevance of T-type calcium-ion channels: potential indications for T-type calcium antagonists. Clin. Ther. *19*, 18–26.

Iwashima, Y., Pugh, W., Depaoli, A.M., Takeda, J., Seino, S., Bell, G.I., and Polonsky, K.S. (1993). Expression of calcium channel mRNAs in rat pancreatic islets and downregulation after glucose infusion. Diabetes *42*, 948–955.

Jowett, T., and Lettice, L. (1994). Whole-mount in situ hybridizations on zebrafish embryos using a mixture of digoxigenin- and fluorescein-labelled probes. Trends Genet. *10*, 73–74.

Kimmel, C.B., Ballard, W.W., Kimmel, S.R., Ullmann, B., and Schilling, T.F. (1995). Stages of embryonic development of the zebrafish. Dev. Dyn. *203*, 253–310.

Knapik, E.W., Goodman, A., Ekker, M., Chevrette, M., Delgado, J., Neuhauss, S., Shimoda, N., Driever, W., Fishman, M.C., and Jacob, H.J. (1998). A microsatellite genetic linkage map for zebrafish (Danio rerio). Nat. Genet. *18*, 338–343.

Lee, R.K., Stainier, D.Y., Weinstein, B.M., and Fishman, M.C. (1994). Cardiovascular development in the zebrafish. II. Endocardial progenitors are sequestered within the heart field. Development *120*, 3361–3366.

Lehmann-Horn, F., and Jurkat-Rott, K. (1999). Voltage-gated ion channels and hereditary disease. Physiol. Rev. *79*, 1317–1372.

MacLellan, W.R., and Schneider, M.D. (2000). Genetic dissection of cardiac growth control pathways. Annu. Rev. Physiol. *62*, 289–319.

Majumdar, A., and Drummond, I.A. (1999). Podocyte differentiation in the absence of endothelial cells as revealed in the zebrafish avascular mutant, cloche. Dev. Genet. *24*, 220–229.

Mangold, O. (1933). Ueber die Induktionsfaehigkeit der verschiedenen Bezirke der Neurula von Urodelen. Naturwissenschaften *21*, 761–766.

Marban, E. (1999). Molecular Basis of Cardiovascular Disease (companion text to E. Braunwald's Heart Disease), K.R. Chien, ed., J. Breslow, J. Leiden, R. Rosenberg, and C.E. Seidman, section eds. (Cambridge, MA: W.B. Saunders).

Mellstrom, B., and Naranjo, J.R. (2001). Ca(2+)-dependent transcriptional repression and derepression: DREAM, a direct effector. Semin. Cell Dev. Biol. *12*, 59–63.

Michelmore, R.W., Paran, I., and Kesseli, R.V. (1991). Identification of markers linked to disease-resistance genes by bulked segregant analysis: a rapid method to detect markers in specific genomic regions by using segregating populations. Proc. Natl. Acad. Sci. USA *88*, 9828–9832.

Molkentin, J.D., Lu, J.R., Antos, C.L., Markham, B., Richardson, J., Robbins, J., Grant, S.R., and Olson, E.N. (1998). A calcineurin-dependent transcriptional pathway for cardiac hypertrophy. Cell *93*, 215–228.

Nattel, S., and Li, D. (2000). Ionic remodeling in the heart: pathophysiological significance and new therapeutic opportunities for atrial fibrillation. Circ. Res. *87*, 440–447.

Nguyen-Tran, V.T.B., Chen, J., Ruiz-Lozano, P., and Chien, K.R. (1999). Genetic control of muscle gene expression. In Heart Development, R.P. Harvey and N. Rosenthal, eds. (San Diego: Academic Press), pp. 255–272.

Pelster, B., and Burggren, W.W. (1996). Disruption of hemoglobin oxygen transport does not impact oxygen-dependent physiological processes in developing embryos of zebra fish (Danio rerio). Circ. Res. *79*, 358–362.

Platzer, J., Engel, J., Schrott-Fischer, A., Stephan, K., Bova, S., Chen, H., Zheng, H., and Striessnig, J. (2000). Congenital deafness and sinoatrial node dysfunction in mice lacking class D L-type Ca2+ channels. Cell *102*, 89–97.

Ramesh, V., Kresch, M.J., Katz, A.M., and Kim, D.H. (1995). Characterization of Ca(2+)-release channels in fetal and adult rat hearts. Am. J. Physiol. *269*, H778–H782.

Sedmera, D., Pexieder, T., Hu, N., and Clark, E.B. (1998). A quantitative study of the ventricular myoarchitecture in the stage 21–29 chick embryo following decreased loading. Eur. J. Morphol. *36*, 105–119.

Seidman, J.G., and Seidman, C. (2001). The genetic basis for cardiomyopathy: from mutation identification to mechanistic paradigms. Cell *104*, 557–567.

Seisenberger, C., Specht, V., Welling, A., Platzer, J., Pfeifer, A., Kuhbandner, S., Striessnig, J., Klugbauer, N., Feil, R., and Hofmann, F. (2000). Functional embryonic cardiomyocytes after disruption of

the L-type α1C (Cav1.2) calcium channel gene in the mouse. J. Biol. Chem. *275*, 39193–39199.

Shistik, E., Keren-Raifman, T., Idelson, G.H., Blumenstein, Y., Dascal, N., and Ivanina, T. (1999). The N terminus of the cardiac L-type Ca(2+) channel α(1C) subunit. The initial segment is ubiquitous and crucial for protein kinase C modulation, but is not directly phosphorylated. J. Biol. Chem. *274*, 31145–31149.

Stainier, D.Y., Fouquet, B., Chen, J.N., Warren, K.S., Weinstein, B.M., Meiler, S.E., Mohideen, M.A., Neuhauss, S.C., Solnica-Krezel, L., Schier, A.F., Zwartkruis, F., Stemple, D.L., Malicki, J., Driever, W., and Fishman, M.C. (1996). Mutations affecting the formation and function of the cardiovascular system in the zebrafish embryo. Development *123*, 285–292.

Striessnig, J. (1999). Pharmacology, structure and function of cardiac L-type Ca(2+) channels. Cell. Physiol. Biochem. *9*, 242–269.

Takimoto, K., Li, D., Nerbonne, J.M., and Levitan, E.S. (1997). Distribution, splicing and glucocorticoid-induced expression of cardiac α 1C and α 1D voltage-gated Ca2+ channel mRNAs. J. Mol. Cell. Cardiol. *29*, 3035–3042.

Tanabe, T., Beam, K.G., Powell, J.A., and Numa, S. (1988). Restoration of excitation-contraction coupling and slow calcium current in dysgenic muscle by dihydropyridine receptor complementary DNA. Nature *336*, 134–139.

van Haasteren, G., Li, S., Muda, M., Susini, S., and Schlegel, W. (1999). Calcium signalling and gene expression. J. Recept. Signal Transduct. Res. *19*, 481–492.

Viatchenko-Karpinski, S., Fleischmann, B.K., Liu, Q., Sauer, H., Gryshchenko, O., Ji, G.J., and Hescheler, J. (1999). Intracellular Ca2+ oscillations drive spontaneous contractions in cardiomyocytes during early development. Proc. Natl. Acad. Sci. USA *96*, 8259–8264.

Westerfield, M. (1995). The Zebrafish Book: A Guide for the Laboratory Use of Zebrafish Danio rerio (Eugene, OR: University of Oregon Press).

Zhong, T.P., Kaphingst, K., Akella, U., Haldi, M., Lander, E.S., and Fishman, M.C. (1998). Zebrafish genomic library in yeast artificial chromosomes. Genomics *48*, 136–138.

Zuhlke, R.D., Pitt, G.S., Deisseroth, K., Tsien, R.W., and Reuter, H. (1999). Calmodulin supports both inactivation and facilitation of L-type calcium channels. Nature *399*, 159–162.

Accession Numbers

The GenBank accession number for the zebrafish C-LTCC sequence reported in this paper is AF305689.